SUB | NIEDERSÄCHSISCHE STAATS- UND UNIVERSITÄTSBIBLIOTHEK GÖTTINGEN

Werk

Jahr: 1976
Kollektion: fid.geo
Signatur: 8 Z NAT 2148:42
Digitalisiert: Niedersächsische Staats- und Universitätsbibliothek Göttingen
Werk Id: PPN1015067948_0042
PURL: http://resolver.sub.uni-goettingen.de/purl?PPN1015067948_0042

LOG Id: LOG_0026
LOG Titel: Rayleigh channel waves for the in-seam seismic detection of discontinuities
LOG Typ: article

Übergeordnetes Werk

Werk Id: PPN1015067948
PURL: http://resolver.sub.uni-goettingen.de/purl?PPN1015067948
OPAC: http://opac.sub.uni-goettingen.de/DB=1/PPN?PPN=1015067948

Terms and Conditions

The Goettingen State and University Library provides access to digitized documents strictly for noncommercial educational, research and private purposes and makes no warranty with regard to their use for other purposes. Some of our collections are protected by copyright. Publication and/or broadcast in any form (including electronic) requires prior written permission from the Goettingen State- and University Library.
Each copy of any part of this document must contain there Terms and Conditions. With the usage of the library's online system to access or download a digitized document you accept the Terms and Conditions.
Reproductions of material on the web site may not be made for or donated to other repositories, nor may be further reproduced without written permission from the Goettingen State- and University Library.

For reproduction requests and permissions, please contact us. If citing materials, please give proper attribution of the source.

Contact

Niedersächsische Staats- und Universitätsbibliothek Göttingen
Georg-August-Universität Göttingen
Platz der Göttinger Sieben 1
37073 Göttingen
Germany
Email: gdz@sub.uni-goettingen.de

J. Geophys. 42, 111 – 129, 1976

Journal of Geophysics

Rayleigh Channel Waves for the In-Seam Seismic Detection of Discontinuities

L. Dresen and S. Freystätter

Institut für Geophysik der Ruhr-Universität Bochum, Postfach 2148, D-4630 Bochum-Querenburg, Federal Republic of Germany

Abstract. Two-dimensional seismic models are used to reproduce the geological sequence cheek-seam-cheek in deep coal mines. The known reflection method based on Rayleigh channel waves is investigated with respect to discontinuities being composed of a termination of the seam and a fractured zone outside the seam. By means of fractured zones having different reflection coefficients discontinuities are designed representing clay hogs or microtectonic faults. Results obtained by investigating amplitudes, frequencies and phase velocities show a strong increase of the rate of amplitude decay with decreasing phase velocity. Furthermore it is demonstrated that the part of the Rayleigh channel wave propagating outside the seam is responsible for the detectability of a discontinuity. Expressing the detectability numerically the ratio E_R of the channel wave's energy inside the seam to its total energy has been used. The value 0.5 for E_R is derived to be a standard value for distinguishing the phase velocity range for which reliable reflection surveys are possible ($E_R > 0.5$) or not ($E_R < 0.5$).

Key words: Detection of discontinuities in deep coal mines – Rayleigh channel waves – Reflection method – Model seismic experiments.

1. Introduction

1.1. The In-Seam Seismic Detection Methods

The increasing mechanisation of coal winning methods and hence the confinement to few intensively exploited coal seams essentially requires the knowledge of the field in front of the operating face. A variety of methods have been examined to predict discontinuities of the coal seam, e.g. microtectonic faults, clay hogs, jamas etc., in front of the operating face. Seismic methods have turned out to be the most promising ones (Baule, 1967). Applying seismic waves in mines for prediction means to use channel waves. As coal has low body wave velocities

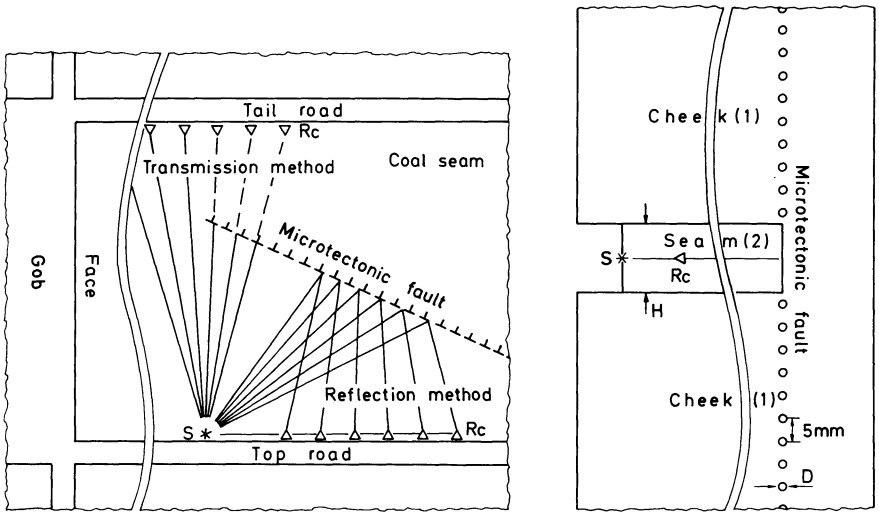

Fig. 1. Experimental set-up in a deep coal mine (left hand side) and on a two-dimensional model (right hand side). *S* seismic source, R_c Receiver

compared with the cheek – i.e. the rock above and below the seam – channel waves can be generated by a seismic source inserted in the coal. Channel waves propagate along the coal seam and can clearly be recorded at distances as far as 1.5 km from the source (Arnetzl, 1971).

Two methods used for predicting discontinuities are based on channel waves. These methods are to observe channel waves reflected from the discontinuity or to observe the distortion of channel waves being transmitted past the discontinuity (cf. left hand side of Fig. 1). The reflection method has the advantage that it yields not only the presence of a discontinuity but also its location. Therefore this paper will primarily be concerned with the reflection method.

Although the fundamental ideas of the in-seam seismic detection of discontinuities and successful applications have been published (Krey, 1963; Arnetzl, 1971) the method sometimes fails. In these cases of failure it has not been possible to find out whether this failure is due to the properties of channel waves or due to improper field procedures (Brentrup, 1970).

1.2. Properties of the Rayleigh Channel Wave

One of the ways to study the fundamental properties of channel waves is to carry out experiments using seismic models. Two-dimensional seismic models can be used to investigate Rayleigh channel waves and three-dimensional ones to investigate Love and Rayleigh channel waves simultaneously. Because two-dimensional models enable us to record the seismic signal at any distance from the source they are a powerful tool to investigate channel waves in the neighbourhood of a reflecting discontinuity. Thus in this paper the behaviour of the Rayleigh channel wave is described.

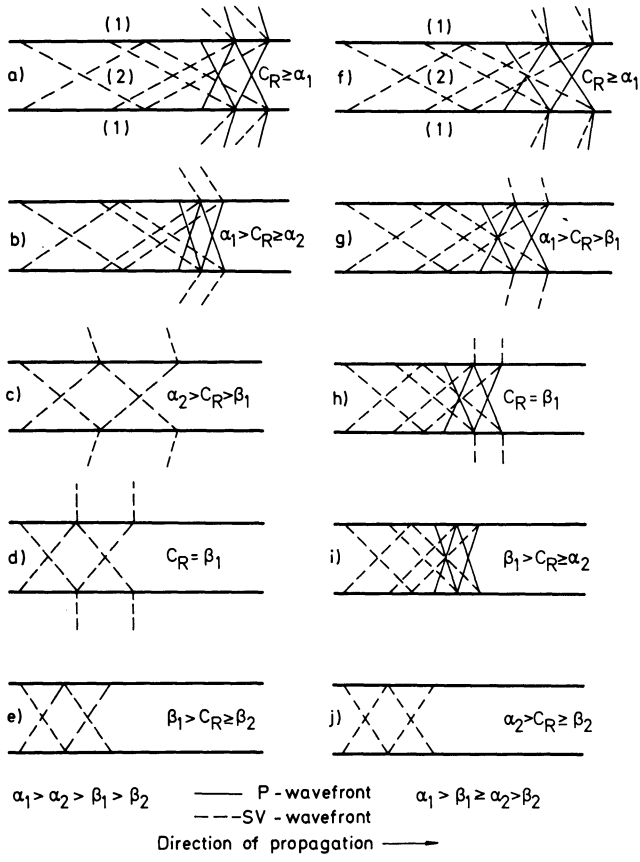

Fig. 2. Wave front patterns of the symmetrical Rayleigh channel wave

In nature the P-wave velocity in the coal α_2 may be higher or lower than the SV-wave velocity in the cheek β_1. Thus two orderings of the body wave velocities are possible:

i) $\alpha_1 > \alpha_2 > \beta_1 > \beta_2$

ii) $\alpha_1 > \beta_1 \geqq \alpha_2 > \beta_2$,

where α_1 is the P-wave velocity in the cheek and β_2 is the SV-wave velocity in the coal.

Since seam thicknesses in West-Europe are commonly smaller than 2 m the lowest possible – so-called fundamental – mode is of interest. Since furthermore the sequence cheek-seam-cheek modelled by means of two-dimensional seismic techniques (cf. right hand side of Fig. 1) represents a symmetrical low velocity channel the fundamental mode is the first symmetrical mode.

Depending upon the relationship of the phase velocity C_R of the Rayleigh channel wave to each of the body wave velocities there may exist leaking or normal modes. The normal modes are important for the application discussed. The wave front patterns a–c and f–g in Figure 2 represent the leaking mode domain and interference patterns d–e and h–j represent the normal mode domain. According

to the interference patterns d and h we have to expect some portions of the normal mode domain's seismic signal being composed of the channel wave and the critically refracted SV-wave. According to our observations the critically refracted SV-wave can have a predominant influence.

Referring to Figure 2 we find that two situations can exist for normal modes of the Rayleigh channel wave: If $\beta_1 \geqq C_R \geqq \alpha_2$ PP-, PSV- and SVSV-reflections occur at the roof and the floor (cf. interference patterns h and i). If $\alpha_2 > C_R \geqq \beta_2$ the normal mode involves only SVSV-reflections (cf. interference patterns d, e and j). Figure 2 shows that the body wave velocity ordering $\alpha_1 > \alpha_2 > \beta_1 > \beta_2$ yields only the latter type of interference pattern within the normal mode domain whereas the ordering $\alpha_1 > \beta_1 \geqq \alpha_2 > \beta_2$ yields both types of interference patterns within the normal mode domain.

1.3. Questions Arising in the Use of Rayleigh Channel Waves for the In-Seam Seismic Detection

For studying the behaviour of the Rayleigh channel wave during its propagation from the source to the discontinuity and from the discontinuity to the receiver the two-dimensional model shown on the right part of Figure 1 is used. This model represents the simplest geometry found in nature namely a seam embedded between two homogeneous, isotropic rock halfspaces. The model contains a discontinuity normal to the stratification. This discontinuity can represent a clay hog as well as a microtectonic fault. Since microtectonic faults have the property that they do not only terminate the seam but are also accompanied by a fractured zone in the cheek being filled with mylonite a single row of holes has been inserted above and below the end of the model seam. Various diameters D of the holes were used. So for $D = 0$ mm the model represents a seam terminated by a clay hog whereas for $D > 0$ mm microtectonic faults having fractured zones with different elastic properties are investigated.

Concerning the case $D = 0$ mm model investigations had been carried out by Freystätter (1974). His results showed that only a portion of the direct Rayleigh channel wave belonging to the normal mode domain is reflected by the discontinuity.

Thus the following question arises:

i) For what range of phase velocities will normal mode waves be reflected by a clay hog or a microtectonic fault?

Freystätter (1974) also showed that even a high value for the absorption of the low velocity coal layer will not seriously effect the shape of the dispersion curve. However we expect a change in the properties of the channel wave along the path of propagation.

This leads to another question:

ii) What sort of change can be expected for the amplitude, phase velocity and frequency of that portion of the direct channel wave which contributes the main energy to the reflected wave?

Answering these questions we have investigated the behaviour of the Rayleigh channel wave along its travel path and at the discontinuity of the seam by means of a number of two-dimensional models.

Some important preliminary measurements concerning materials and modelling the discontinuity are described in Section 2. The results of the model experiments are given in Section 3. Conclusions will follow in Section 4.

2. Details of the Model Seismic Technique and Models Used

2.1. Equipment

The equipment is similar to the one commonly used for the analogue recording model seismograms gained with the ultrasonic transducer technique (e.g. O'Brien and Symes, 1971; Behrens and Waniek, 1972; Dresen, 1972). Due to the possibility of expanding any portion of the seismic signal the set-up used allows a maximum accuracy for analogue recording (Freystätter, 1974). The mean square error produced by the complete set-up amounts to $\pm 2\%$ with respect to phase velocity measurements, $\pm 3\%$ with respect to frequency measurements and $\pm 6\%$ with respect to amplitude measurements.

2.2. Materials

Concerning the cheek in all cases an Aluminium plate has been used as model material (cf. Table 1).

In modelling the case $\alpha_1 > \alpha_2 > \beta_1 > \beta_2$ we found only Pertinax® to be a useful material for the seam. As Pertinax is made of several layers of paper coated with phenol resin and the tensile strength of the paper varies with the direction of strain the material is not isotropic. The body wave velocity distribution measured in Pertinax equals the one of an ideal transversely isotropic material (Postma, 1955) within $\pm 2\%$.

In modelling the case $\alpha_1 > \beta_1 \geqq \alpha_2 > \beta_2$ we solved the problem of finding a material with a P-wave velocity close to the SV-wave velocity in Aluminium by filling epoxy resin – or its derivative the glue Araldite® – with tiny glass balls (Ballotini®) which have a diameter of 75 μm to 150 μm. Different rates of filler

Table 1. Parameters of the model materials. The dimension [mm/μs] used for the models equals the dimension [km/s] used for in-situ measurements

	P-wave velocity α [mm/μs]	SV-wave velocity β [mm/μs]	Density ρ [g/cm^3]	Absorption coefficient a_A [dB/λ]
Aluminium	5.44	3.13	2.7	<0.01
Pertinax	parallel to strike:		1.4	0.65
	4.12	2.18		
	perpendicular to strike:			
	3.3	2.18		
Araldite + Ballotini (1:2)	2.86	1.72	1.63	0.9
Epoxy Resin + Ballotini (1:2)	2.86	1.72	1.63	0.85
Plexiglas	2.33	1.36	1.2	0.7

enable the fabrication of materials with P-wave velocities in the range of approximately 2 mm/μs to approximately 3 mm/μs. The advantage of this composed material is not only the wide range of body wave velocities but also the non-necessity of an additional bonding layer between the materials for seam and cheek. Besides this we have used the classic model material Plexiglas® for the seam.

The combined use of transversely isotropic and isotropic materials does not affect the interpretation by means of dispersion curves calculated according to Anderson (1971). One of the conspicuous properties of the low velocity channel to be investigated is the high absorption contrast between seam and cheek. We may assume the cheek to have an absorption constant between 0.01 and 0.1 dB/λ whereas the absorption constant of coal has the order of magnitude of 1 dB/λ. We can generally say that the comparison of the model materials' parameters with the values occuring in nature (Schwaetzer and Desbrandes, 1965; Baule, 1967) show an appreciable correspondence.

2.3. *Models*

Properties of the models determining the frequency range of the generated Rayleigh channel wave are given in Table 2. I.e. the predominant frequency f_p

Table 2. Parameters of models used. Aluminium has been taken to model the cheek. The dimension [kHz · mm] used for the model measurements equals the dimension [Hz · m] used for in-situ measurements

Materials for the series of models investigated	Code number for the series of models investigated	Predominant frequency of the seismic source f_p [kHz]	Thickness of low-velocity layer (coal seam) H [mm]	Length of low-velocity layer (coal seam) L [mm]	Source-Receiver Distance		Reflector-Receiver Distance	
					x_A [mm]	x_B [mm]	x_C [mm]	x_D [mm]
Aluminium/ Pertinax	0312	108	12.6±0.3	785	160	680	105	615
Aluminium/ Araldite + Ballotini (1:2)	0506	108	6.2±0.2	770	200	520	50	570
Aluminium/ Epoxy Resin + Ballotini (1:2)	0409	108	9.5±0.3	780	200	600	140	580
Aluminium/ Araldite + Ballotini (1:2)	0518	108	18.7±0.3	770	240	760	130	610
Aluminium/ Plexiglas	0106	108	6.9±0.2	770	240	720	170	570
Aluminium/ Plexiglas	0115	108	15.1±0.3	780	280	720	180	580

of the model seismic source and the thickness H of the low velocity layer (coal seam). The length L of the low velocity layer is given too. It follows that the ratio L/H is similar to the situation given in a coal mine.

Furthermore the different investigated series of models have been coded such that the first two figures characterize the material combination and the last two figures characterize the thickness of the seam. Each series of models includes one model containing no fractured zone in the cheek and three models containing a fractured zone with D equals 2 mm, 3 mm and 4 mm.

The source-receiver distances and reflector-receiver distances give the limitations of the range within the records have been evaluated. They will be discussed in paragraph 4.1.

2.4. Experimental Determination of Reflection Coefficients

To get an idea of the influence of the fractured zone on the reflection process of Rayleigh channel waves taking place at the discontinuity of the seam we have experimentally determined the reflection coefficients at different types of reflectors. For this determination we used the amplitudes of the direct and reflected nondispersive Rayleigh wave propagating normal to the reflector.

The reflection coefficients valid for a single row of holes having a diameter of 2 mm, 3 mm and 4 mm are given in Table 3, line 1 to 3. For comparison the reflection coefficient valid for a thin bonding layer (thickness approximately 0.3 mm) between two Aluminium plates has been measured (cf. Table 3, line 4). According to these results the reflection coefficients valid for fractured zones represented by a row of holes lie in the same order of magnitude as the reflection coefficient valid for the sequence Aluminium/thin bonding layer/Aluminium which is, with respect to its shape, a more typical fractured zone.

Table 3. Reflection coefficients at various reflectors determined by means of the nondispersive Rayleigh wave

	Type of reflector	Reflection coefficients		Remarks
		Component perpendicular to the reflector	Component parallel to the reflector	
1	Aluminium plate containing a single row of holes $D=2$ mm	0.23 ± 0.03	0.16 ± 0.01	The distances between the holes' centres equal 5 mm
2	Aluminium plate containing a single row of holes $D=3$ mm	0.50 ± 0.05	0.36 ± 0.01	
3	Aluminium plate containing a single row of holes $D=4$ mm	0.72 ± 0.08	0.57 ± 0.02	
4	Aluminium/Aluminium Bonding material: Araldite	0.58 ± 0.06	0.40 ± 0.02	The thickness of the bonding layer equals ca. 0.3 mm
5	Plexiglas/Aluminium Bonding material: Araldite	0.42 ± 0.08	0.40 ± 0.04	

However the advantage of the hole-drilling technique is the possibility of producing a set of different fractured zones having reliably reproducible reflection coefficients by means of simply changing the diameter of the holes.

Moreover the reflection coefficient of the materials at the termination of the seam, like e.g. Plexiglas and Aluminium, can be assumed to lie within the range of reflection coefficients valid for the various fractured zones (cf. Table 3, line 5). Hence follows that cases with both relatively low and relatively high influence of the fractured zone are covered by our models. Thus the models correspond with the geological situation in deep coal mines.

3. Model Experiments Concerning Direct and Reflected Rayleigh Channel Waves

3.1. General Remarks

In this part the questions

i) For what range of phase velocities will normal mode waves be reflected by a clay hog or a microtectonic fault?

and

ii) What sort of change can be expected for the amplitude, phase velocity and frequency of that portion of the direct channel wave which contributes the main energy to the reflected wave?

will be answered by means of model experiments. The answer of question ii) will be based on measured values. The answer of question i) however will be based on the mean square errors of these measured values. Therefore we shall firstly discuss question ii) and thereupon question i).

As the features of the reflection process are of main interest the properties of both the direct and the reflected normal mode signal have been investigated. According to the evaluation of analogously recorded signals the oscillation of the direct channel wave with the maximum double amplitude has been evaluated (Fig. 3). Concerning the reflected wave the portion corresponding to the mentioned oscillation of the direct wave with the maximum double amplitude has been evaluated. It should be pointed out that this portion does not always contain the maximum double amplitude of the reflected wave's signal. As an example Figure 3 contains a single seismogram measured for a source-receiver distance of 660 mm (cf. total seismogram section in Fig. 9 b). The signal's portions I, II, III and III_r are labelled "wave groups" and correspond to different parts of the dispersion curve (cf. Freystätter, 1974).

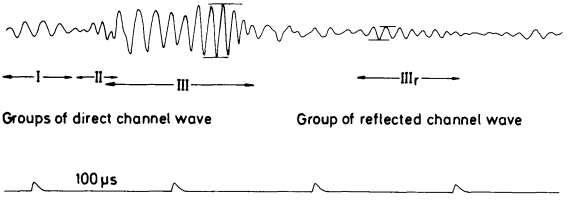

Fig. 3. Seismogram containing several groups of Rayleigh channel waves

The measurements of the direct wave's properties were carried out within the source-receiver distances x_A and x_B and the one's of the reflected wave were carried out within the reflector-receiver distances x_C and x_D (cf. Table 2). These limitations had to be chosen because of the superposition of different wave groups close to the source and close to the receiver.

3.2. Rate of Amplitude Decay

Due to the measurements being carried out on each model of a model series we have derived average values for the rate of amplitude decay between x_A and x_B and x_C and x_D respectively. The decay of the amplitude of both the direct and the reflected wave has been proved to be approximately an exponential one. This has led us to dimension the rate of decay in dB/H thus getting a constant for a given model. Hence follows the equation defining the rate of amplitude decay a of the direct wave:

$$a[\mathrm{dB}/H] = \left| 20 \cdot \frac{\log A(x_B) - \log A(x_A)}{x_B - x_A} \right|$$

where x_A and x_B are expressed in units of H (thickness of the coal seam). A similar equation is valid describing the rate of amplitude decay a_r within the range between the reflector-receiver distances x_C and x_D.

Referring to Table 4 we find the numerical values of a and a_r distinctly differing. For the series of models 0506, 0409, 0518, 0106 and 0115 – representing the body wave velocity ordering $\alpha_1 > \beta_1 \geqq \alpha_2 > \beta_2$ – the ratio a_r/a lies between 0.6 and 0.7. I.e. the rate of amplitude decay of the direct wave is clearly higher than the one of the reflected wave.

Concerning the model series 0312 – representing the body wave velocity ordering $\alpha_1 > \alpha_2 > \beta_1 > \beta_2$ – the numerical values of a and a_r distinctly differ too, yet this time the rate of amplitude decay of the direct wave is clearly lower than the one of the reflected wave.

Table 4. Coefficients of the Rayleigh channel wave yielded by means of model seismic measurements

Code number for the series of models investigated	Rate of amplitude decay			Rate of frequency change			Rate of phase velocity change		
	Direct channel wave a [dB/H]	Reflected channel wave a_r [dB/H]	Ratio a_r/a	Direct wave b [dB/H]	Reflected wave b_r [dB/H]	Ratio b_r/b	Direct wave c [dB/H]	Reflected wave c_r [dB/H]	Ratio c_r/c
0312	0.015	0.022	1.5	−0.048	−0.0079	0.2	0.0027	0.0019	0.7
0506	0.085	0.06	0.7	−0.017	−0.0035	0.2	0.0011	0.0027	2.5
0409	0.16	0.089	0.6	−0.025	−0.0059	0.25	0.0024	0.0018	0.8
0518	0.24	0.17	0.7	−0.067	−0.034	0.5	0.0058	0.0097	1.7
0106	0.22	0.13	0.6	−0.022	−0.0078	0.4	0.003	0.0011	0.4
0115	0.33	0.23	0.7	−0.028	−0.021	0.8	0.0081	0.0062	0.8

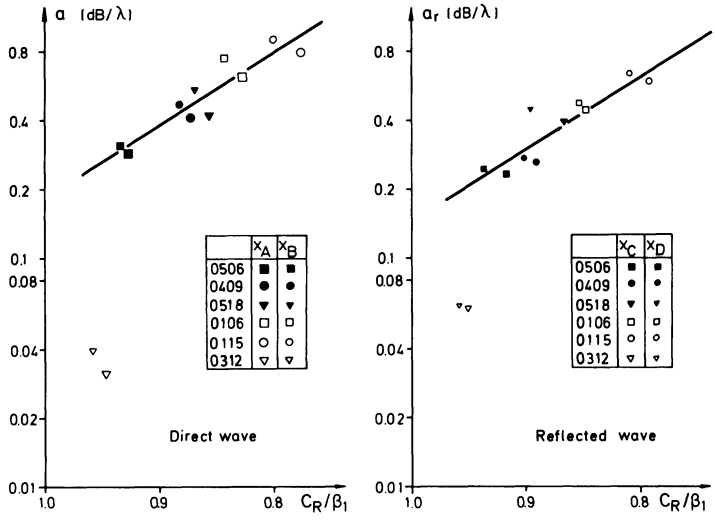

Fig. 4. Amplitude decay of the Rayleigh channel wave

The absolute values of the rate of amplitude decay distinctly differ for the body wave velocity ordering $\alpha_1 > \beta_1 \geqq \alpha_2 > \beta_2$ and the ordering $\alpha_1 > \alpha_2 > \beta_1 > \beta_2$.

Because we know from Table 1 that the absorption coefficients of all materials used for modelling the seam lie in the same order of magnitude, the different values for a or a_r respectively can be explained by the influence of the critically refracted SV-wave (cf. Section 1.2, Fig. 2, pattern d).

For the application of the in-seam seismic detection of discontinuities in deep coal mines it is necessary to get an idea about the rate of amplitude decay depending on the phase velocity C_R of the channel wave or the frequency respectively. This relationship is given in Figure 4 for the measured values of C_R being normalized with β_1 and the values a [dB/λ] or a_r [dB/λ] derived from a [dB/H] or a_r [dB/H] by means of phase velocity and frequency determined for the distances x_A, x_B, x_C and x_D. Figure 4 shows that assuming the body wave velocity ordering $\alpha_1 > \beta_1 \geqq \alpha_2 > \beta_2$ (0506, 0409, 0518, 0106 and 0115) and an order of magnitude of 1 [dB/λ] for the absorption coefficient of body waves in the seam material (cf. Table 1) the rate of amplitude decay of the Rayleigh channel wave strongly increases with decreasing phase velocity. According to the discussed ratio a_r/a the absolute values of a and a_r are different yet the curves slopes coincide. This is understandable because the different absolute values are due to the reflection process whereas the discussed curve's slope is a function of the material constants. According to Table 1 these material constants differ for the investigated series of models. Thus the experimentally derived curve provides an evidence to take the numerical value of its slope for estimating the increase of the rate of amplitude decay of several different material combinations. The value for the model series 0312 representing the velocity ordering $\alpha_1 > \alpha_2 > \beta_1 > \beta_2$ which does not fit into the curves of Figure 4 is due to the predominant influence of the critically refracted SV-waves (refer to Section 1.2).

As in these investigations materials with body wave absorption coefficients similar to those existing in nature have been used we may take the graphs given in Figure 4 as a reliable aid for in-situ measurements in deep coal mines. Thus we may assume the numerical values for the rate of amplitude decay of the Rayleigh channel wave to lie in the range of 0.1 to 1 dB/λ where the geometrically caused spread has still to be taken into account.

3.3. Rate of Frequency Change and Rate of Phase Velocity Change

According to the measurements the frequency change and the phase velocity change proved to be approximately exponential ones, too. Thus the rate of frequency change b of the direct wave and b_r of the reflected wave have been derived from the measured signals analogously to a and a_r:

$$b\,[\mathrm{dB}/H] = 20\,\frac{\log f(x_B) - \log f(x_A)}{x_B - x_A}$$

where f is the predominant frequency of the investigated channel wave portion. x_A and x_B are again expressed in units of H. A similar equation has been used for b_r.

The values of the rate of phase velocity change c of the direct and c_r of the reflected channel wave are gained by means of equations similar to the one for b.

According to Table 4 the numerical values of b, b_r, c and c_r are approximately one and two orders of magnitude smaller than the ones of a and a_r. Thus deter-

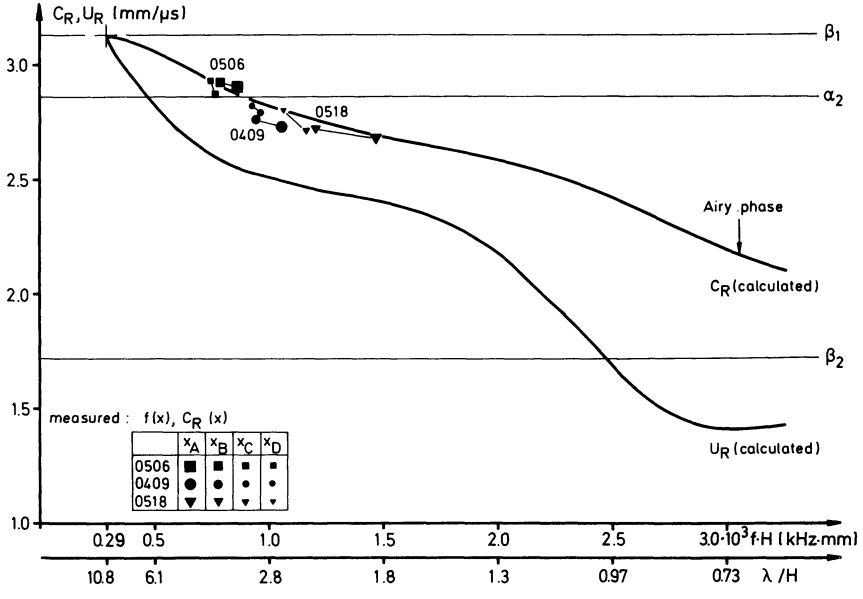

Fig. 5. Comparison between calculated dispersion curves and measured frequency and phase velocity values

mining the absolute values is rather problematic. Only the order of magnitude and the tendency being evident in all measurements is a reliable base for conclusions.

According to this statement the rate of frequency change b or b_r lies between -0.01 dB/H and -0.1 dB/H whereas the rate of phase velocity change c or c_r lies between $+0.001$ dB/H and $+0.01$ dB/H. The negative sign of b and b_r indicates a decreasing frequency with increasing source-receiver distance and reflector-receiver distance respectively. The positive signal of c and c_r indicates an increasing phase velocity with increasing source-receiver and reflector-receiver distance respectively. This means that the properties of the Rayleigh channel wave's portion being of interest for the in-seam seismic detection method changes along the travel path. In other words the point representing the measurements for a certain source-receiver distance "moves" along the dispersion curve from relatively low phase velocities and high frequencies towards higher phase velocities and lower frequencies (Fig. 5). Hence follows that the group velocity changes along the travel path, too. Thus an error has to be taken into account in determining the discontinuity's distance to the operating face.

The order of magnitude of b, b_r, c and c_r and the tendency determined are easily understood in comparing the measured results with the phase velocity dispersion curve. Concerning the model series 0506, 0409 and 0518 this is shown in Figure 5. For comparison the calculated group velocity U_R has been drawn, too.

3.4. Reflection Coefficient and the Reflecting Discontinuity

The measured reflection coefficients R for each series of models are depicted in Figure 6. According to Figure 6 the continually increasing diameter D of the holes in the cheek which represent the fractured zone leads to a series of increasing reflection coefficients for each series of models. How can this be explained?

This can be explained by means of the channel wave's part propagating outside the seam. To support this statement we have calculated the displacement

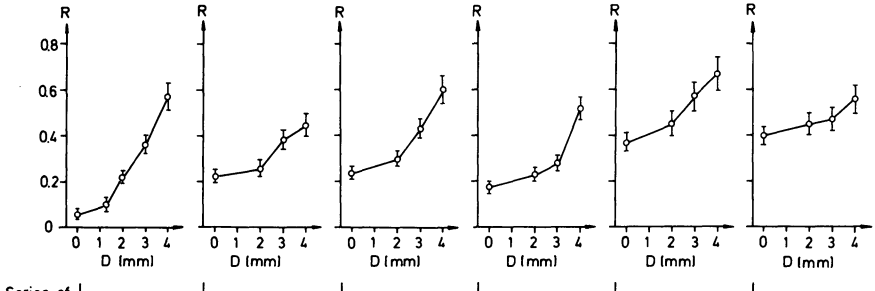

Series of models	0312	0506	0409	0518	0106	0115
α_1/α_2	1.3 *	1.9	1.9	1.9	2.3	2.3

*α_2 parallel to strike

Fig. 6. Reflection coefficient of various discontinuities with respect to the Rayleigh channel wave

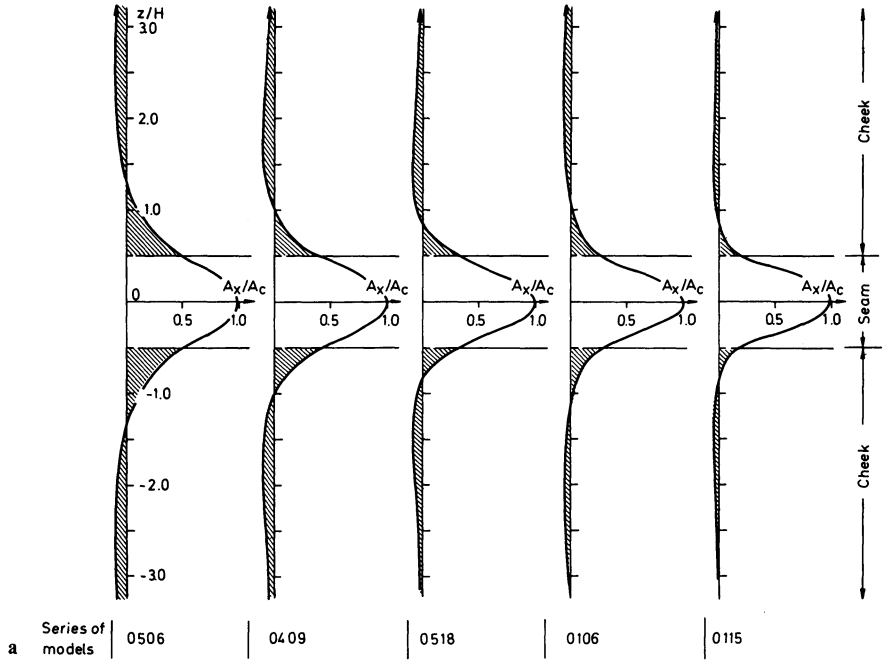

a

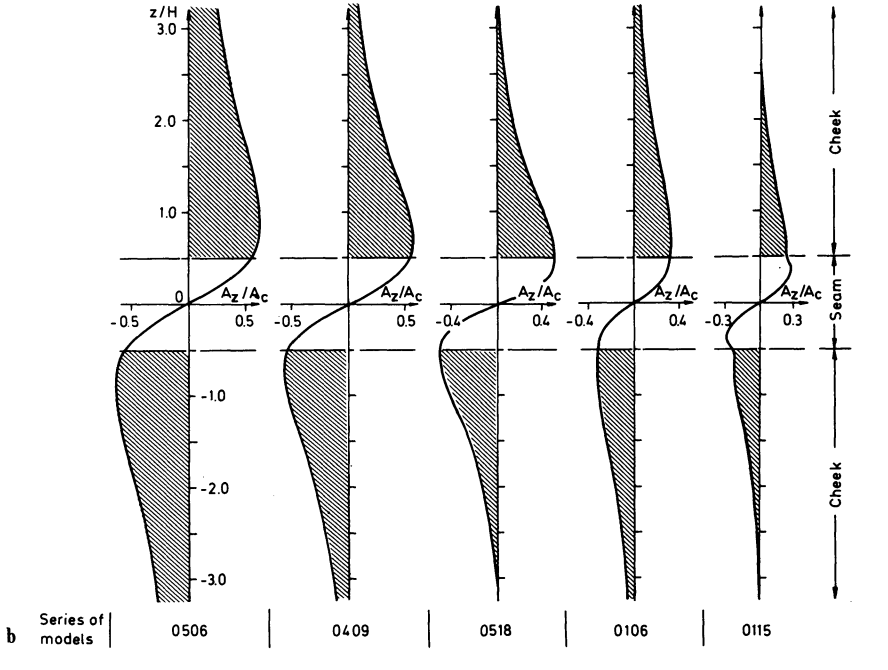

b

Fig. 7a–b. Amplitude distribution of Rayleigh channel waves along the sequence cheek-seam-cheek

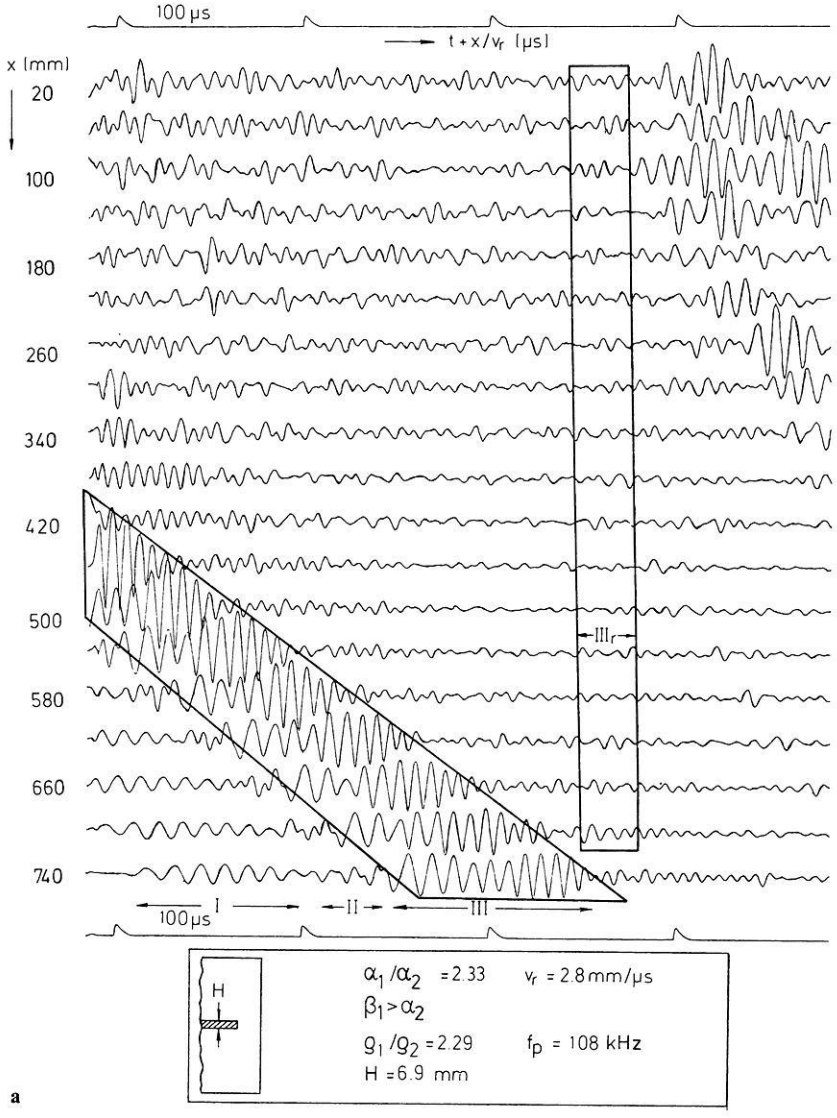

Fig. 8a–b. Seismogram section of the direct (wavegroups I, II, III) and the reflected (wavegroup III_r) Rayleigh channel wave

amplitude distribution (cf. Freystätter, 1974) for the Rayleigh channel wave using the experimentally determined phase velocity and frequency at the reflecting discontinuity. The results for the amplitudes parallel (A_x) and perpendicular (A_z) to the stratification are given in Figure 7a–b. Both amplitudes have been normalized with the maximum amplitude A_c parallel to the stratification in the centre-plane. According to Figure 7a–b the amplitudes of the Rayleigh channel wave outside the seam are not negligible with respect to the reflection process in presence of a fractured zone.

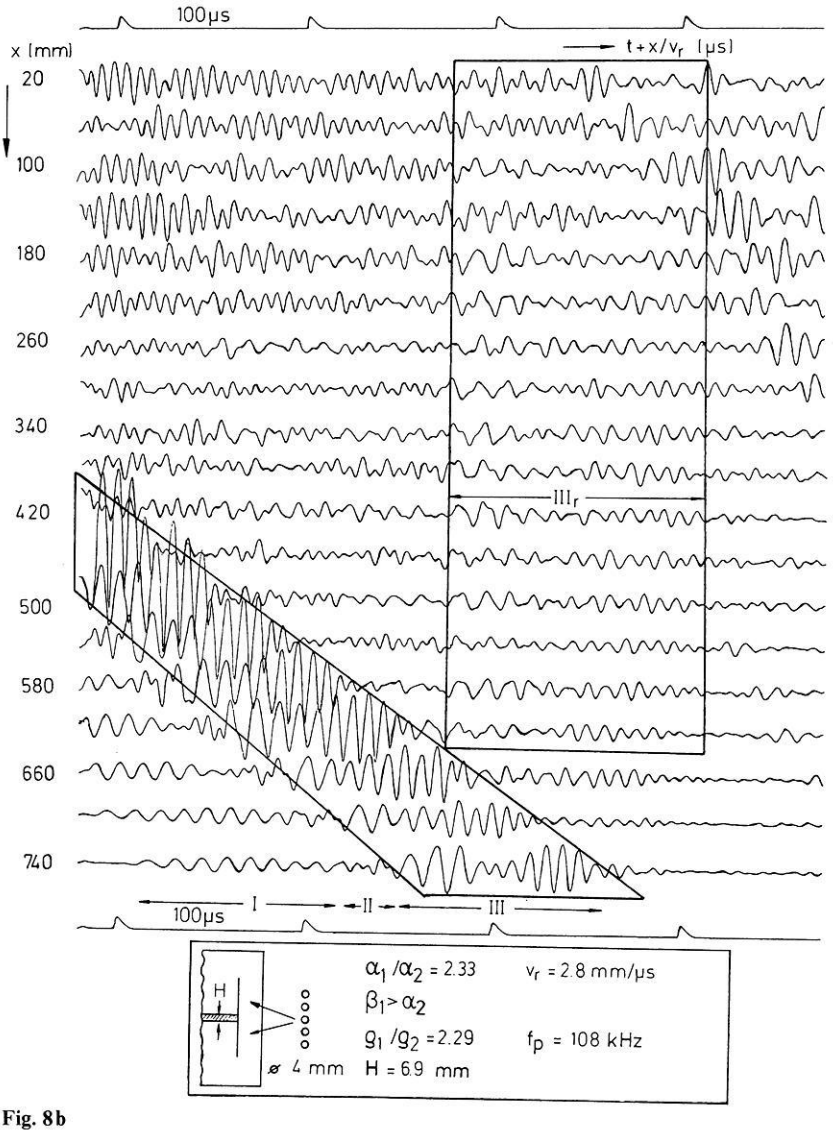

Fig. 8b

Discussing the reflection coefficients for the case $D = 0$ mm – i.e. a discontinuity without a fractured zone – we find the trend of increasing reflection coefficients R with increasing P-wave velocity contrast α_1/α_2 (cf. Fig. 6). This is confirmed by distinct steps of R from the model series 0312 to the series 0506, 0409 and 0518 and again from these three series to the series 0106 and 0115.

Discussing the reflection coefficients measured with all series of models for the case $D = 4$ mm this distinct stepwise behaviour cannot be observed. According to the results listed in Table 3 we expect the reflection coefficient for a single row

of holes with $D=4$ mm to be higher than the reflection coefficient for the interface of the material combination with the highest P-wave velocity contrast namely Plexiglas and Aluminium. We thus explain the result found for the case $D=4$ mm such that the influence of the velocity contrast on the reflection coefficient R has decreased in favour of the influence of the fractured zone.

From these observed results follows that the reflection coefficient for a Rayleigh channel wave at a discontinuity depends on the P-wave velocity contrast and on the existence of a fractured zone in the cheek accompanying the discontinuity. Additionally to this the development of the fractured zone influences the reflection coefficient, too. This means for in-situ measurements that clay hogs will have lower reflection coefficients than microtectonic faults.

3.5. The Detectability of the Reflected Channel Wave

So far only the behaviour of the direct channel wave's portion with the maximum double amplitude and the appropriate reflected channel wave's portion have been discussed. Yet the distinction with which the total reflected wave appears in the seismograms i.e. its detectability has not been quantitatively investigated.

To gain a qualitative impression of the reflected channel wave's shape Figure 8a–b contain seismogram sections for the model series 0106. The models with which the seismograms have been gained only differ in the type of fractured zone due to $D=0$ mm and $D=4$ mm. According to Figure 6 this means an increase of the reflection coefficient from $R=0.37$ for the case $D=0$ mm to $R=0.67$ for the case $D=4$ mm. I.e. approximately a doubling of the reflected channel wave's amplitudes. Moreover comparing the signals of the reflected channel wave in Figure 8a–b we find for $D=4$ mm the length of the reflected wave's signal distinctly increased which is due to the existence of the fractured zone. Thus its detectability has increased, too.

To estimate the detectability quantitatively the amplitudes' mean square error σ_a of the investigated reflected channel wave's portion has been determined with respect to the amplitude decay curve. Similar quantities for the frequencies (σ_b) and phase velocities (σ_c) have been determined with respect to the frequency change curve and phase velocity change curve respectively. For comparison the mean square errors δ_a, δ_b, δ_c of the appropriate direct wave's portion between the source-receiver distances x_A and x_B have been calculated. From these quantities the integral quantity σ_N was calculated as follows

$$\sigma_N = \pm \tfrac{1}{3} \left(\left| \frac{\sigma_a}{\delta_a} \right| + \left| \frac{\sigma_b}{\delta_b} \right| + \left| \frac{\sigma_c}{\delta_c} \right| \right).$$

The corresponding parameter δ_N for the direct channel wave equals ± 1 according to

$$\delta_N = \pm \tfrac{1}{3} \left(\left| \frac{\delta_a}{\delta_a} \right| + \left| \frac{\delta_b}{\delta_b} \right| + \left| \frac{\delta_c}{\delta_c} \right| \right).$$

In Figure 9 the values of σ_N and δ_N are depicted for each model series. The upper hatched area between $|\sigma_N|$ and $|\sigma_N| - |\delta_N|$ represents the values of $|\sigma_N|$ expected

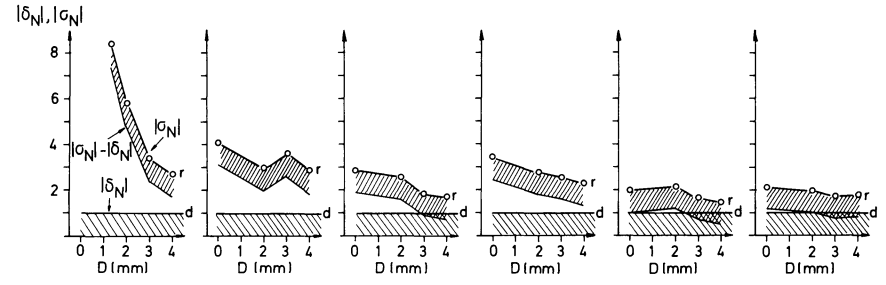

Series of models	0312	0506	0409	0106	0518	0115
E_R	0.1	0.16	0.3	0.34	0.42	0.6

Fig. 9. Detectability σ_N of the reflected Rayleigh channel wave

for a measurement. The lower hatched area represents the values of $|\delta_N|$. It is evident that the fractured zone in the cheek influences the detectability of the reflected channel wave. This means according to the shape of the amplitude curves described in Section 3.4 that the part of the channel wave propagating outside the seam plays an important role for the detectability of the reflected channel wave.

It has to be pointed out, that σ_N is a quantity only for model investigations where the modelled geological situation is known. This means σ_N will only provide a tool for in-situ measurements if we are able to combine its information with a measure which can be calculated for a given field case.

For such a measure the energy ratio E_R was defined:

$$E_R = \int_{-H/2}^{+H/2} \int_0^T \tfrac{1}{2}\rho(v_x^2 + v_z^2)\,\mathrm{d}z\,\mathrm{d}t \Big/ \int_{-\infty}^{+\infty} \int_0^T \tfrac{1}{2}\rho(v_x^2 + v_z^2)\,\mathrm{d}z\,\mathrm{d}t.$$

The numerator expresses the kinetic energy over one period T which is transported inside the seam with the thickness H by the Rayleigh channel wave whereas the denominator expresses the kinetic energy over one period T which is transported inside and outside the seam. The quantity ρ is the density and the quantities v_x and v_z are the particle velocities parallel and perpendicular to the stratification. The integration over the second coordinate y has not been mentioned as the results of both numerator and denominator equal each other. Knowing the parameters of cheek and seam – i.e. elastic moduli, densities and thickness of the layer – and taking the commonly used potentials of a symmetrical channel wave we can calculate the quantity E_R without referring to special in-situ measurements.

The numerical values of E_R calculated for the investigated channel wave's portion are given in Figure 9. Comparing the values for E_R and the behaviour of the $|\sigma_N|$ curve for each model series we find for E_R below 0.42 or 0.6 respectively the distinct tendency of a decrasing $|\sigma_N|$ with increasing D. I.e. the detectability of the reflected wave clearly depends on the distinction of the fractured zone. For E_R equals 0.42 or 0.6 this tendency is very weak and the detectability of both channel waves reflected by clay hogs and channel waves reflected by micro-

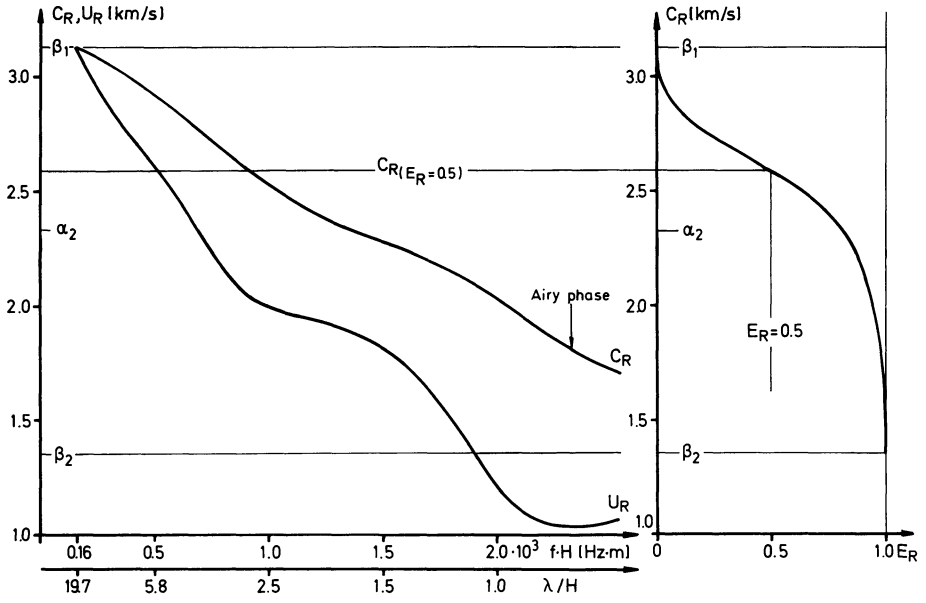

Fig. 10. Example of determining the range of phase velocities useful for the reflection method using Rayleigh channel waves

tectonic faults is similar. Furthermore according to the relatively close neighbourhood of both hatched areas we expect a good detectability for these discontinuities. According to this the value 0.5 for E_R seams to us to be a useful standard value for distinguishing that part of the Rayleigh channel wave being reliable with respect to the reflection method from the impracticable one.

Figure 10 demonstrates for body wave velocity values equal to those of the models 0106 and 0115 how the confinement given by E_R equals 0.5 divides the dispersion curve into two parts. Within the upper one we cannot expect reliable results with respect to the existence or non-existence of discontinuities. Yet within the lower one we may expect to yield results which can reliably be used to determine a discontinuity inside a coal seam.

4. Conclusions

In this paper the principle usefulness of Rayleigh channel waves with respect to the in-seam seismic reflection method has been investigated by means of two-dimensional seismic models. For this purpose the simplest model for a coal seam has been chosen namely a symmetrical low velocity channel. Likewise the simplest type of discontinuity in a coal seam has been chosen too i.e. a complete cut-off normal to the stratification. Furthermore the influence of a fractured zone in the cheek accompanying the discontinuity has been taken into account. Thus models of the two most common discontinuities – namely clay hogs and microtectonic faults – have been investigated. At the beginning of this paper we have formulated two questions the answers of which we will compile in a comprehended form:

Concerning the Rayleigh channel wave reflected by a discontinuity we have found that the part of the channel wave propagating outside the seam plays an important role. To rely on a good detectability of the reflected channel wave it is necessary to choose a phase velocity range where this part outside the seam is so small that the numerical value of the ratio E_R between the channel wave's energy in the seam and the channel wave's total energy will preferably be higher than the standard value 0.5. Thus we recommend, prior to the use of Rayleigh channel waves for a given in-situ case to determine the elastic moduli for coal and cheek. With these values the relevant energy ratio curves can be calculated such that a successful use of the Rayleigh channel wave can be estimated.

Concerning the behaviour of that portion of the Rayleigh channel wave which contributes the main energy to the reflected channel wave we have found that the absorption coefficient rapidly increases with decreasing phase velocity. Frequency and phase velocity changes of the portion mentioned above could be observed too. These changes exactly behave as it is expected according to the shape of the phase velocity dispersion curve. In due course we have to consider a change of the group velocity along the travel path of both the direct and the reflected Rayleigh channel wave. Determining the distances between the reflecting discontinuity and the operating coal face this change of the group velocity has to be taken into account.

Acknowledgement. We are indebted to Dr. R. Schepers for stimulating discussions and critically reading the manuscript. The investigation has been carried out under DFG-contract no. Dr 110/2.

References

Anderson, D. L.: Elastic wave propagation in layered anisotropic media. J. Geophys. Res. **66**, 2953–2963, 1961

Arnetzl, H.: Seismische Messungen unter Tage. Tagungsbericht der Gesellschaft deutscher Metallhütten- und Bergleute, 8.5. 1971, S. 133–141

Baule, H.: Vorfelderkundung mit geophysikalischen Mitteln. Mitt. a.d. Markscheidewesen **74**, 205–228, 1967

Behrens, J., Waniek, L.: Modellseismik. Z. Geophys. **38**, 1–44, 1972

Brentrup, F.-K.: Seismische Vorfelderkundung zur Ortung tektonischer Störungen im Steinkohlenbergbau. Glückauf **106**, 933–938, 1970

Dresen, L.: Modellseismische Untersuchungen zum Problem der Ortung oberflächennaher kreiszylindrischer Hohlräume in Festgestein, Berichte des Institutes für Geophysik der Ruhr-Universität Bochum, Nr. 1, Bochum 1972

Freystätter, S.: Modellseismische Untersuchungen zur Anwendung von Flözwellen für die untertägige Vorfelderkundung im Steinkohlenbergbau, Berichte des Institutes für Geophysik der Ruhr-Universität Bochum, Nr. 3, Bochum, 1974

Krey, T.: Channel waves as a tool of applied geophysics in coal mining. Geophysics **28**, 701–714, 1963

O'Brien, P. N. S., Symes, M. P.: Model seismology. Reports on Progress in Physics **34**, 697–764, 1971

Postma, G. W.: Wave propagation in a stratified medium. Geophysics **20**, 780–806, 1955

Schwaetzer, T., Desbrandes, R.: Divergences constatées dans la mesure de la vitesse des ondes acoustiques longitudinales du charbon. Revue Inst. Française Petrol **20**, 3–26, 1965

Received December 4, 1975